

Nuclear structure with accurate chiral perturbation theory nucleon-nucleon potential: Application to ${}^6\text{Li}$ and ${}^{10}\text{B}$

P. Navrátil

Lawrence Livermore National Laboratory, L-414, P.O. Box 808, Livermore, CA 94551

E. Caurier

*Institut de Recherches Subatomiques (IN2P3-CNRS-Université Louis Pasteur)
Batiment 27/1, 67037 Strasbourg Cedex 2, France*

We calculate properties of $A = 6$ system using the accurate charge-dependent nucleon-nucleon (NN) potential at fourth order of chiral perturbation theory. By application of the *ab initio* no-core shell model (NCSM) and a variational calculation in the harmonic oscillator basis with basis size up to $16\hbar\Omega$ we obtain the ${}^6\text{Li}$ binding energy of 28.5(5) MeV and a converged excitation spectrum. Also, we calculate properties of ${}^{10}\text{B}$ using the same NN potential in a basis space of up to $8\hbar\Omega$. Our results are consistent with results obtained by standard accurate NN potentials and demonstrate a deficiency of Hamiltonians consisting of only two-body terms. At this order of chiral perturbation theory three-body terms appear. It is expected that inclusion of such terms in the Hamiltonian will improve agreement with experiment.

PACS numbers: 21.60.Cs, 21.45.+v, 21.30.-x, 21.30.Fe

I. INTRODUCTION

A new development in the theory of nuclear forces occurred when the concept of an effective field theory (EFT) was introduced and applied to the low-energy QCD [1]. Starting from a general Lagrangian consistent with the QCD symmetries, in particular the broken chiral symmetry, one can develop a systematic perturbative expansion valid at low energies for effective degrees of freedom, nucleons and pions. Pioneering work in this direction was performed by Ordonez, Ray and van Kolck [2, 3] who constructed a nucleon-nucleon (NN) potential in the coordinate space based on the chiral perturbation theory at the third order. Similarly, Epelbaum *et al.* [4] developed the first momentum space NN potential at the third order of the chiral perturbation theory. Recently, Entem and Machleidt developed an EFT based momentum space non-local NN potential at the fourth order of the chiral perturbation theory (next-to-next-to-next-to-leading order, N^3LO) [5] that takes into account the charge dependence and fits the two-nucleon data with similar accuracy as the traditional phenomenological high-quality NN potentials like Argonne V18 [6] or the CD-Bonn 2000 [7].

It is an important question and a test for the EFT approach how well these new potentials will describe the nuclear structure of light nuclei when applied to more than two nucleons. The new accurate N^3LO NN potential is a non-local momentum-space potential. There are several methods that could be applied to solve $A = 3, 4$ systems using this potential, most notably the Faddeev and the Faddeev-Yakubovsky techniques [8]. However, the best established method for obtaining exact results for the $A > 4$ p -shell nuclei, the Green's Function Monte Carlo (GFMC) approach [9, 10, 11], is not applicable as it is best suited for work with local coordinate space potentials like AV18 or AV8' [12]. The N^3LO potential can be used, however, in the *ab initio* no-core shell model approach (NCSM) [13]. In this method, we perform calculations in a finite harmonic-oscillator (HO) basis using effective interactions appropriate to the basis size truncation that are systematically derived from the original inter-nucleon potential. The method is convergent to the exact solution with the basis size enlargement and/or with the degree of clustering of the effective interaction. Due to the properties of the HO basis it is no technical problem to use either local or non-local and either coordinate or momentum space potentials.

In this paper, we apply the NCSM to obtain nuclear structure results using the N^3LO NN potential for ${}^3\text{H}$, ${}^4\text{He}$, ${}^6\text{Li}$, ${}^6\text{He}$ and ${}^{10}\text{B}$. With the improved shell model code ANTOINE [14, 15] we are able to reach basis sizes up to the $16\hbar\Omega$ for ${}^6\text{Li}$ and up to the $8\hbar\Omega$ for ${}^{10}\text{B}$. At the same time, we perform variational calculations in the HO basis for ${}^6\text{Li}$ using the bare N^3LO potential. These variational calculations allow us to make extrapolations and check our NCSM effective interaction results. In addition, we compare the N^3LO results to those obtained by the CD-Bonn 2000 and the AV8'.

It should be pointed out that already at the third order of the chiral perturbation theory, N^2LO , three-body terms appear [16]. These terms should be consistently included in calculations for $A > 2$ nuclei. It is our goal to perform the NCSM calculations with the three-body terms included using the approach outlined in Ref. [17]. In fact, work in

this direction is under way [18]. However, in general when only the two-nucleon interactions are employed the NCSM approach can achieve a higher accuracy as larger basis spaces can be reached. Therefore, it is valuable to perform accurate calculations using just the two-nucleon forces to assess the effects of the omitted three-nucleon terms. The eventual less accurate results obtained with both the two- and three-nucleon forces can then be better understood and extrapolated.

We briefly review the basic features of the NCSM and describe our variational calculations in the HO basis in Section II. In Section III, we present our N³LO results for ³H and ⁴He. In Section IV, we discuss our calculations for $A = 6$ using the N³LO NN potential and compare them to results obtained by the AV8' and the CD-Bonn 2000. In addition, we check convergence properties of our approach using the semi-realistic Minnesota NN potential. In Section V, we show the NCSM predictions for ¹⁰B with the N³LO NN potential. Our conclusions are summarized in Section VI.

II. *AB INITIO* NO-CORE SHELL MODEL AND VARIATIONAL CALCULATIONS IN THE HO BASIS

A detailed description of the NCSM approach was presented, e.g. in Refs. [13, 22, 23]. Here we only briefly review the basic features of the NCSM. Also, we describe our variational calculations in the HO basis that we apply in the following Sections.

The starting Hamiltonian for our investigations is

$$H_A = \frac{1}{A} \sum_{i < j}^A \frac{(\vec{p}_i - \vec{p}_j)^2}{2m} + \sum_{i < j}^A V_{\text{NN},ij}, \quad (1)$$

where m is the nucleon mass, $V_{\text{NN},ij}$, the NN interaction with both strong and electromagnetic components. In the NCSM, we employ a large but finite harmonic-oscillator (HO) basis. Due to properties of the realistic nuclear interaction in Eq. (1), we must derive an effective interaction appropriate for the basis truncation in order to reach convergence or to achieve a reasonable approximation to the exact solution. To facilitate the derivation of the effective interaction, we modify the Hamiltonian (1) by adding to it the center-of-mass (CM) HO Hamiltonian $H_{\text{CM}} = T_{\text{CM}} + U_{\text{CM}}$, where $U_{\text{CM}} = \frac{1}{2}Am\Omega^2\vec{R}^2$, $\vec{R} = \frac{1}{A}\sum_{i=1}^A\vec{r}_i$. This modification was first introduced by Lipkin [19]. The effect of the HO CM Hamiltonian will later be subtracted out in the final many-body calculation. Due to the translational invariance of the Hamiltonian (1) the HO CM Hamiltonian has in fact no effect on the intrinsic properties of the system in the infinite basis space or in a finite basis space truncated by N_{max} as described below if the interaction in Eq. (1) is not altered.

The modified Hamiltonian can be cast into the form

$$\begin{aligned} H_A^\Omega &= H_A + H_{\text{CM}} = \sum_{i=1}^A h_i + \sum_{i < j}^A V_{ij}^{\Omega,A} \\ &= \sum_{i=1}^A \left[\frac{\vec{p}_i^2}{2m} + \frac{1}{2}m\Omega^2\vec{r}_i^2 \right] + \sum_{i < j}^A \left[V_{\text{NN},ij} - \frac{m\Omega^2}{2A}(\vec{r}_i - \vec{r}_j)^2 \right]. \end{aligned} \quad (2)$$

Next we divide the A -nucleon infinite HO basis space into the finite active space (P) comprising of all states of up to N_{max} HO excitations above the unperturbed ground state and the excluded space ($Q = 1 - P$). The basic idea of the NCSM approach is to apply a unitary transformation on the Hamiltonian (2), $e^{-S}H_A^\Omega e^S$ such that $Qe^{-S}H_A^\Omega e^S P = 0$ [24, 25]. If such a transformation is found, the effective Hamiltonian that exactly reproduces a subset of eigenstates of the full space Hamiltonian is given by $H_{\text{eff}} = Pe^{-S}H_A^\Omega e^S P$. This effective Hamiltonian contains up to A -body terms and to construct it is essentially as difficult as to solve the full problem. Therefore, we apply this basic idea on a sub-cluster level. In this paper we use the simplest approximation, a two-body effective interaction approximation. This approximation is obtained by constructing the unitary transformation for the Hamiltonian (2) applied to two nucleons only, i.e., $\mathcal{H}_2 = h_1 + h_2 + V_{12}^{\Omega,A}$ with A in $V_{12}^{\Omega,A}$ fixed at the value corresponding to the final A -nucleon calculation. The two-body effective interaction is then derived with the help of the exact eigensolutions of \mathcal{H}_2 as $[V_{12}^{\Omega,A}]_{\text{eff}} = P_2 [e^{-S_2}\mathcal{H}_2 e^{S_2} - h_1 - h_2] P_2$. Here, the definition of the two-nucleon model space projector P_2 follows directly from the definition of the A -nucleon projector P . The two-nucleon transformation S_2 is determined by the condition $Q_2 e^{-S_2}\mathcal{H}_2 e^{S_2} P_2 = 0$.

The A -nucleon calculation with $A > 4$ is then performed using the multi-shell (no-core) version of the code AN-

TOINE, with the Hamiltonian in the form:

$$H_{A,\text{eff}}^{\Omega,\text{SM}} = P \left\{ \sum_{i<j}^A \left[\frac{(\vec{p}_i - \vec{p}_j)^2}{2Am} + \frac{m\Omega^2}{2A}(\vec{r}_i - \vec{r}_j)^2 \right] + \sum_{i<j}^A \left[V_{\text{NN},ij} - \frac{m\Omega^2}{2A}(\vec{r}_i - \vec{r}_j)^2 \right]_{\text{eff}} + \beta(H_{\text{CM}} - \frac{3}{2}\hbar\Omega) \right\} P, \quad (3)$$

where we subtracted the CM Hamiltonian H_{CM} and added the Lawson projection term $\beta(H_{\text{CM}} - \frac{3}{2}\hbar\Omega)$ to shift the spurious CM excitations. As our effective interaction is translationally invariant our physical eigenenergies do not depend on the choice of β . Note that in Section III we present $A = 3, 4$ calculations performed in Jacobi coordinate antisymmetrized HO basis. In those calculations the CM degrees of freedom are explicitly omitted and therefore no $\beta(H_{\text{CM}} - \frac{3}{2}\hbar\Omega)$ term is used.

We note that our effective interaction depends on the nucleon number A , the HO frequency Ω , and the P -space basis size defined by N_{max} . It is translationally invariant and with $N_{\text{max}} \rightarrow \infty$ the NCSM effective Hamiltonian approaches the starting bare Hamiltonian (1). Consequently, with the basis size increase the NCSM results become less and less dependent on the HO frequency and converge to the exact solution. Alternatively, by increasing the clustering of the effective interaction for a fixed P -space size the NCSM effective Hamiltonian approaches the exact A -nucleon effective Hamiltonian that reproduces exactly a subset of eigenstates of the starting Hamiltonian (1).

It turns out that the N^3LO NN potential is softer than the phenomenological high-quality NN potentials like the AV18 or the CD-Bonn. As we are able to reach basis spaces of up to $N_{\text{max}} = 18$ and $N_{\text{max}} = 16$ for $A = 4$ and $A = 6$, respectively, it make sense to perform variational calculations in the HO basis for ${}^4\text{He}$ and ${}^6\text{Li}$ using the bare N^3LO NN potential with the HO frequency or the oscillator length as the only variational parameter. In this case, the Hamiltonian that we use is PH_AP , with H_A given in Eq. (1) (plus the $\beta P(H_{\text{CM}} - \frac{3}{2}\hbar\Omega)P$ term when Slater determinant basis is utilized, i.e., for $A > 4$). We perform variational calculations for different basis sizes defined by N_{max} . We then extrapolate to $N_{\text{max}} \rightarrow \infty$ and compare to our effective interaction results.

III. ${}^3\text{H}$ AND ${}^4\text{He}$ RESULTS

As a test of convergence of our method and also as a test of correct interfacing of our codes with the N^3LO NN potential code [20] we performed calculations for ${}^3\text{H}$ and ${}^4\text{He}$. We used the translationally invariant HO basis antisymmetrized as described in Ref. [23] and employed the many-body effective interaction code MANYEFF [23]. Our results are summarized in Table I. Our ${}^3\text{H}$ binding energy, 7.85(1) MeV, that was obtained using basis spaces up to $N_{\text{max}} = 40$ agrees well with the result obtained by the Faddeev method [20].

Our ${}^4\text{He}$ binding energy calculations were performed using both bare and the two-body effective interactions in basis spaces up to $N_{\text{max}} = 18$. Our obtained binding energy, 25.36(4) MeV, is very close to that obtained by the Faddeev-Yakubovsky method [18]. In Fig. 1, we present the HO frequency dependence of our ${}^4\text{He}$ binding energy for different basis sizes. Calculations with two-body effective interactions are compared to the variational calculations using the bare N^3LO NN potential. The NCSM calculations with the two-body effective interaction are not variational as some terms of the transformed Hamiltonian (i.e., the higher than two-body terms) are omitted. Therefore, in the NCSM approach the convergence could be, depending on the HO frequency, either from above or below or even oscillatory with the basis size enlargement. It should be noted how the frequency dependence of our ${}^4\text{He}$ binding energy decreases with the basis size enlargement. Also, the two-body effective interaction always improves on the bare interaction results in particular for the smaller spaces and lower HO frequencies. For example, the $N_{\text{max}} = 14$ ($14\hbar\Omega$) binding energy obtained using the effective interaction varies within 25.11 MeV and 25.5 MeV in the range of HO frequencies shown in Fig. 1, $\hbar\Omega = 24 - 40$ MeV. The bare interaction binding energy in the same basis space and the same frequency range varies within 23.09 MeV and 25.12 MeV. For the highest frequency that we used here, $\hbar\Omega = 40$ MeV, we observe that the improvements due to the two-body effective interaction become very small. We note that the the minimum of the variational calculation in the $N_{\text{max}} = 18$ basis space is at about $\hbar\Omega = 36$ MeV. The minima for the smaller space calculations are at still higher frequencies, e.g., the minimum of the of the $N_{\text{max}} = 12$ calculation is at $\hbar\Omega > 40$ MeV outside of the range shown in Fig. 1. At $N_{\text{max}} = 18$ our effective interaction calculations agree with the variational bare interaction result.

It is instructive to investigate in addition to the binding energy also the convergence of the point-nucleon ${}^4\text{He}$ radius. A similar plot as in Fig. 1 is presented for the point-nucleon root mean square radius in Fig. 2. Even though no operator renormalization was used for the radius operator very similar conclusions can be drawn as for the binding energy. The calculation with the effective interaction (i.e., with wave functions obtained using the effective interactions) improves convergence and reduces the frequency dependence compared to a calculation with the bare interaction wave functions using the same basis size. With the basis enlargement the frequency dependence decreases. At the same time, it should be noticed that the optimal frequency for the radius convergence is not necessarily the

same as that for the binding energy. It is important to investigate the frequency dependence of energies and other observables to determine the extrapolated values and errors. We extrapolate the ${}^4\text{He}$ radius with the N^3LO potential to be 1.515(10) fm. In Fig. 3 we show the complete basis size dependence of the point-nucleon radius calculation using the effective interaction for several HO frequencies. The convergence with N_{max} and the decrease of frequency dependence can be clearly seen.

The ${}^3\text{H}$ and ${}^4\text{He}$ N^3LO binding energies (7.85 MeV, 25.36 MeV) are in between the Argonne V8' (7.77 MeV, 25.2 MeV) and the CD-Bonn binding energies (8.00 MeV, 26.3 MeV) but considerably closer to the AV8' results. Note that the Coulomb interaction is included for all three potentials.

IV. APPLICATION TO ${}^6\text{Li}$ AND ${}^6\text{He}$

As mentioned earlier, our $A = 6$ calculations reported here were obtained using the improved multi-shell (no-core) version of the code ANTOINE capable to reach basis spaces up to $N_{\text{max}} = 16$ ($16\hbar\Omega$) for ${}^6\text{Li}$ with the M-scheme basis dimension equal to 8×10^8 . A specific challenge of the no-core calculations compared to the traditional $0\hbar\Omega$ valence nucleon calculations is the enormous number of single particle states (e.g., there are 171 nlj levels and 2280 $nljm$ states for each protons and neutrons in the $16\hbar\Omega$ ${}^6\text{Li}$ calculations). This implies a huge number of operators that need to be stored in memory. The other challenge is the huge dimension of the matrix to be diagonalized. Both these challenges have been addressed in the improved ANTOINE code. In particular, an efficient way of operator storage was found and a partitioning of Lanczos vectors was introduced that eliminates the need to store the full Lanczos vectors in memory.

Before presenting our N^3LO results, let us first discuss test calculations for ${}^6\text{Li}$ using the semi-realistic Minnesota (MN) NN potential [26] frequently used for few-body calculation benchmarks [27, 28]. Our NCSM results, in particular the HO frequency dependence of the ground-state energy for different basis spaces ranging from $N_{\text{max}} = 0$ to $N_{\text{max}} = 14$, are presented in Fig. 4. Clearly, for the Minnesota NN potential we observe the best case scenario of the NCSM convergence. Starting from $N_{\text{max}} = 2$ the convergence is uniform in the whole frequency range. The HO frequency dependence is getting weaker with the basis size enlargement. The differences between the successive curves decrease as the basis size increases. At $N_{\text{max}} = 14$ the NCSM energy at the minimum is within 30 keV of the Stochastic Variational Method (SVM) [27] result 36.51 MeV [29]. An $N_{\text{max}} = 16$ calculation improves the NCSM and SVM agreement to 10 keV. Similarly, the Effective Interaction in the Hyperspherical Harmonics basis (EIHH) method [28, 30] obtains a very close binding energy of 36.64(7) MeV [31]. Let us mention that a variational calculation in the HO basis using the bare Minnesota NN potential still misses about 1.5 MeV from the converged value in the $N_{\text{max}} = 14$ basis space. The improvement due to the two-body effective interaction is quite dramatic even for such a large basis space. The Minnesota NN potential was employed as a test potential for the NCSM ${}^6\text{Li}$ investigation already in Ref. [32]. There, however, basis spaces up to only $N_{\text{max}} = 10$ were utilized. Also, the Minnesota NN potential results presented in Ref. [32] include the Coulomb interaction which was omitted in the present calculations.

We now turn to our ${}^6\text{Li}$ N^3LO results. In Fig. 5, we present the HO frequency dependence of the ground-state energy obtained by the variational calculations (dashed lines) in $N_{\text{max}} = 8$ to $N_{\text{max}} = 16$ basis spaces and by the two-body effective interaction NCSM calculations in basis spaces ranging from $N_{\text{max}} = 2$ to $N_{\text{max}} = 14$. The variational calculations exhibit large changes with N_{max} and clearly they are not converged at $N_{\text{max}} = 16$. The minimum in the largest spaces that we used develops at about $\hbar\Omega = 33$ MeV and the value at minimum for the $N_{\text{max}} = 16$ space is -24.7 MeV. The NCSM two-body effective interaction results (full lines in Fig. 5) show stronger HO frequency dependence than those obtained using the Minnesota NN potential and in fact also than those obtained using the CD-Bonn NN potential [32]. We can see that the minimum appears around $\hbar\Omega = 12$ MeV and shifts with increasing N_{max} to lower frequency. Due to this shift the successive curves intersect and we do not have a nice uniform picture as in the case of the Minnesota interaction. At the same time, the value at minimum does not change much starting at $N_{\text{max}} = 6$ as can be seen in Fig. 6 where we plot the ground-state energy obtained at the minimum for each N_{max} . It is interesting to note that for the largest spaces, e.g. $N_{\text{max}} = 14$, a second minimum develops at around the frequency where the bare interaction results are at the minimum. Similarly as in the case of ${}^4\text{He}$, we can see that starting at certain frequency, the two-body effective interaction does not change the bare interaction results any more and the effective interaction curves start to follow the bare interaction curves.

In Fig. 6, we also present the bare interaction variational calculation results at fixed HO frequencies at or close to the minimum of the $N_{\text{max}} = 14$ and $N_{\text{max}} = 16$ spaces. It turns out that these ground-state energy N_{max} dependencies can be fitted by an exponential function of the type $E(N_{\text{max}}) = E_{\infty} + ae^{-bN_{\text{max}}}$ (see an analogous fit done for the hyperspherical harmonics basis calculation in Ref. [28]). When we fit this formula to the last four points, $N_{\text{max}} = 8 - 16$, we obtain $E_{\infty} \approx -28.2$ MeV. This is rather close to the energy at the minima of our two-body effective interaction calculations that are at about 28.5 MeV. Based on the variational bare interaction calculations and extrapolation and on the two-body effective interaction NCSM calculations in different spaces and using different

frequencies we arrive at our final ${}^6\text{Li}$ N^3LO binding energy result of 28.5(5) MeV. The experimental ${}^6\text{Li}$ binding energy is 31.995 MeV. Our calculations suggest that the N^3LO NN potential under-binds ${}^6\text{Li}$ by about 3.5 MeV.

It is interesting to compare the N^3LO results to those obtained by other NN potentials. Concerning the binding energy, in Fig. 7 we repeat the basis size dependence from Fig. 6 of the NCSM ground-state energy at the frequency minima for the N^3LO and show the same for the AV8', CD-Bonn 2000 and the Minnesota NN potentials. In addition, the AV8' GFMC result [10] and the Minnesota SVM [29] and EIHH [31] results are shown for comparison. As discussed earlier, our Minnesota results show a nice convergence and agree quite well in particular with the SVM result. Our AV8' binding energy is close to that obtained using the N^3LO NN potential and within about 300 keV of the GFMC result. Our CD-Bonn 2000 binding energy is, on the other hand, larger by almost 1 MeV compared to the N^3LO and the AV8'. Our present result is almost the same as that presented in Ref. [32] using the older version of the CD-Bonn NN potential and the NCSM calculations in basis spaces up to only $10\hbar\Omega$. Our binding energy results are tabulated in Tables II and III with our conservative error estimates based on the frequency and basis size sensitivity.

We investigated the excitation energies of the five lowest excited states of ${}^6\text{Li}$ using the N^3LO NN potential. As the binding energy minimum shifts with the change of the basis size and also as we expect that the energy of different excited states might have different dependence on the HO frequency than the ground state, we calculated the excitation energies for several HO frequencies. Due to the complexity of the calculations, the lowest four states were obtained in basis spaces up to $N_{\text{max}} = 14$ while we stopped at $N_{\text{max}} = 12$ for the 2^+1 and the 1^+_{20} state. The NCSM excitation energy dependence on the basis size is presented in Figs. 8, 9 and 10 for the HO frequencies of $\hbar\Omega = 8, 10$ and 13 MeV, respectively. In Fig. 11, we then show the excitation energies for the $\hbar\Omega = 8, 10, 12$ and 13 MeV HO frequencies in the largest basis space used. It is apparent that the convergence rate with N_{max} is different for different states. In particular, the 3^+0 state and the 0^+1 state converge faster in the higher frequency calculations, while the higher lying states converge faster in the lower frequency calculations. As can be seen from Fig. 11 in the largest space used the dependence on the HO frequency is very weak. We summarize our excitation energies with the estimated errors in Table II. We have, in particular, confidence in our 3^+0 excitation energy that is reflected in a very small associated uncertainty. In the $N_{\text{max}} = 14$ space, the 3^+0 excitation energy is almost frequency independent in the range of $\hbar\Omega = 10 - 13$ MeV. At $\hbar\Omega = 8$ MeV, this state has a slightly higher excitation energy. However, it is seen from Fig. 8 that its energy is still decreasing with the basis size enlargement. On the other hand, this state is fairly stable and converged with N_{max} in the $\hbar\Omega = 10 - 13$ MeV calculations.

In general, our calculated levels are in the correct order when compared to experiment for the lowest four states. Concerning the 2^+1 and the 1^+_{20} state, those are obtained at almost the same energy and the uncertainty of our results is too large to make a definitive prediction as to their ordering. When comparing our results to experiment we notice a striking discrepancy for the 3^+0 state that calculated excitation energy is about 0.7 MeV higher than the experimental one. Taking into account our confidence in convergence of this state, this is a serious discrepancy in the prediction of the N^3LO NN potential. The remaining states, when considering our estimated errors, are in fairly good agreement with experiment. We note, however, a significant underestimation of the splitting between the 3^+0 and the 2^+0 states. This splitting is influenced by the spin-orbit interaction strength.

In Table III, we compare our N^3LO excitation energy results with our NCSM results obtained by the CD-Bonn 2000 and the AV8' NN potentials. In addition, we also present the GFMC ${}^6\text{Li}$ results obtained using the AV8'. We note that we have not performed as detailed excitation energy calculations using the CD-Bonn 2000 and the AV8' as we did for the N^3LO . The presented NCSM CD-Bonn 2000 and the AV8' excitation energies were obtained in the $N_{\text{max}} = 14$ basis space using the HO frequency of $\hbar\Omega = 12$ MeV and $\hbar\Omega = 11$ MeV, respectively. We expect, however, that the error estimates that we found for our N^3LO excitation energy results are also applicable to our tabulated CD-Bonn 2000 and AV8' excitation energy calculations. It is apparent that when considering the estimated uncertainties our NCSM calculations cannot discriminate between the three realistic NN potentials as to their predictions of the excitation energies. The CD-Bonn gives a slightly lower excitation energy of the 3^+0 state and a slightly larger splitting between the 3^+0 and the 2^+0 states. However, the differences are smaller than the difference between our NCSM AV8' and the GFMC AV8' results. In general, the NCSM and the GFMC results using the AV8' are in a reasonable agreement. Although we have an about 200 keV difference in the 3^+0 excitation energy, the difference with respect to experiment is about 800 keV for the NCSM and about 1 MeV for the GFMC. This further supports our statement about the failure of the accurate NN potentials to predict the position of this lowest excited state of ${}^6\text{Li}$.

The ${}^6\text{Li}$ with the CD-Bonn and the AV8' was investigated within the NCSM in Refs. [32, 33] using the basis spaces up to $N_{\text{max}} = 10$ with the two-body effective interaction and $N_{\text{max}} = 6$ with the three-body effective interaction. The results that we present here are consistent with the previously published results. Only the 2^+0 excitation energy reported in this work is better converged and smaller. This is due to the larger basis space, i.e. $N_{\text{max}} = 14$, employed here. We note that there is approximately a 500 keV difference in the excitation energy of the 0^+1 state obtained in the NCSM and the GFMC using the AV8'. It is interesting to point out that the NCSM calculations using the three-body effective interaction in the $N_{\text{max}} = 6$ space predict this 0^+1 state at a higher excitation energy closer to the

GFMC result than the NCSM calculations that employ just the two-body effective interaction in similar basis spaces [33]. This is contrary to the $T = 0$ states excitation energy results that are very similar using both the two-body or the three-body effective interaction [33]. The difference for the 0^+1 state in the two NCSM approximations needs further investigation. Ultimately, with the basis size enlargement the results in both approximations must by construction converge to the same value.

In Table II, we also present electromagnetic properties of ${}^6\text{Li}$, binding energy of ${}^6\text{He}$ and the Gamow-Teller ${}^6\text{He} \rightarrow {}^6\text{Li}$ B(GT) value obtained in our NCSM calculations using the N^3LO NN potential. The ${}^6\text{He}$ binding energy is consistent with our ${}^6\text{Li}$ results and under-binds experiment by about 3 MeV. The NCSM calculated electromagnetic properties, obtained using bare charges, are in a reasonable agreement with experiment. We note that while the B(M1) result is fairly stable with the basis size change the B(E2) values increase in general as the basis size is increased. Consequently, our B(M1) values reported here are almost the same as those published in Ref. [32] but our present B(E2) values are substantially larger. The present results were obtained using $N_{\text{max}} = 14$ while those of Ref. [32] using $N_{\text{max}} = 10$. We note that our B(GT) value for the ${}^6\text{He} \rightarrow {}^6\text{Li}$ ground-state to ground-state transition over-predicts experiment. Recently, Schiavilla and Wiringa found that the AV18/Urbana-IX interaction also over-predicts the ${}^6\text{He} \rightarrow {}^6\text{Li}$ B(GT) value [34]. In fact, their obtained Gamow-Teller matrix elements ($\equiv \sqrt{\text{B(GT)}}$), 2.254(5) and 2.246(10) using two types of wave functions, compare well with our result 2.28 obtained using the N^3LO NN potential.

In order to judge the convergence of other observables than just energies, in Fig. 12 we present the HO frequency dependence of the ${}^6\text{Li}$ ground-state quadrupole moment for different basis sizes. Similar conclusions as for the ${}^4\text{He}$ radius calculations can be drawn here. With the basis size increase the frequency dependence decreases. At the same time, the fastest convergence is not necessarily obtained for the same frequency as for the binding energy. A speed up of convergence for the electromagnetic quadrupole observables should be achieved by using effective operators. This has not been done here, but work on this problem is currently under way [35]. We conclude that the quadrupole moment of ${}^6\text{Li}$ with the N^3LO interaction is $-0.08(2) e \text{ fm}^2$.

To summarize this section, apart from more binding obtained using the CD-Bonn 2000 NN potential, we can see little differences in predictions of the $A = 6$ nuclei properties by the three accurate NN potentials, the N^3LO , the CD-Bonn 2000 and the AV8'. Let us just note that we also investigated the $2\hbar\Omega$ -dominated (intruder) states in ${}^6\text{He}$ (not observed in experiment) using the three NN potentials. Such states observed in heavier p -shell nuclei are in general predicted by the NCSM at too high energies and converge much more slowly than the p -shell dominated states [15, 36]. Using the same basis size and the same HO frequency, these states appear at lower excitation energy when the N^3LO NN potential is used compared to the CD-Bonn 2000 and the AV8'. This does not necessarily imply that the N^3LO NN potential will predict the $2\hbar\Omega$ -dominated states at lower energies but perhaps that the NCSM convergence of such states is faster when the N^3LO NN potential is used.

V. APPLICATION TO ${}^{10}\text{B}$

In the previous section we pointed out that the N^3LO NN potential fails to predict correct excitation energy of the 3^+0 state in ${}^6\text{Li}$ by about 700 keV. It has been realized that this problem which is common to other accurate NN potentials is magnified in ${}^{10}\text{B}$. The ground state of ${}^{10}\text{B}$ is 3^+0 and the 1^+0 state is the ${}^{10}\text{B}$ first excited state at 0.72 MeV. Both the NCSM ${}^{10}\text{B}$ calculations using the CD-Bonn and the Argonne NN potentials and the GFMC ${}^{10}\text{B}$ calculations using the Argonne NN potentials show that these accurate NN potentials predict incorrectly the 1^+0 state as the ground state and the 3^+0 state as an excited state at higher than 1 MeV of excitation energy [11, 33, 36]. This is a clear indication for the need of a three-nucleon force not only to fix the under-binding problem but also to correct, at least in some nuclei like ${}^{10}\text{B}$, the level ordering. In fact, it has already been shown that, e.g., for the AV8' NN potential the ${}^{10}\text{B}$ ground-state spin problem is resolved by including certain types of the three-nucleon forces like Illinois [11] or the Tucson-Melbourne TM'(99) [17], but it is not resolved by including the Urbana IX [11]. This type of sensitivity suggests that nuclear structure calculations for light nuclei could be used to help determine the form and the parametrization of realistic three-nucleon forces that are unlike the two-nucleon interactions not well established.

It is quite interesting to perform the ${}^{10}\text{B}$ calculations using the N^3LO NN potential. Our NCSM results performed in basis spaces up to $N_{\text{max}} = 8$ are presented in Figs. 13 and 14 and Table IV. Unlike in the case of ${}^6\text{Li}$, we were not able to reach as large basis spaces that are needed for the excitation energy or the binding energy convergence. Still, our calculations are sufficient to resolve the ground-state spin issue in ${}^{10}\text{B}$ with the N^3LO NN potential. In Fig. 13, we present the dependence of the ${}^{10}\text{B}$ 1^+0 and 3^+0 state energy on the HO frequency for different model spaces. In the NCSM, one typically determines the optimal HO frequency for the ground state and uses the same frequency to describe the excited states. In general, however, one should also investigate the the frequency dependence for the excited states in order to determine their energy [33]. This is in particular important in the ${}^{10}\text{B}$ investigation when we actually want to find out which state is the ground state for a given NN potential. In the inset of Fig. 13, the 1^+0 and 3^+0 state energies at their respective HO frequency minima are plotted as a function of N_{max} . We can see that

in the whole frequency range that we show the 1^+0 state is always the ground state. For the highest frequency shown in the Figure, $\hbar\Omega = 16$ MeV, the excitation energy of the 3^+0 state becomes quite small. However, we observe that with the basis size increase the 3^+0 excitation energy is actually increasing. In Fig. 14, we then show the excitation energies of the lowest 5 ^{10}B states calculated in the $0\hbar\Omega - 8\hbar\Omega$ basis spaces using a fixed HO frequency of $\hbar\Omega = 12$ MeV. At this frequency, the ground-state energy is at the minimum in the $8\hbar\Omega$ space. Clearly, the excitation spectrum is not converged as it was the case in our ^6Li calculations. However, there is definitely a trend to convergence. The differences between the successive calculations become smaller and smaller with increasing N_{max} . We can conclude with confidence that the 3^+0 state will remain the excited state with further increase of N_{max} and most likely will appear at an excitation energy of more than 1 MeV. Based on our NCSM calculations, we conclude that the N^3LO NN potential fails to produce a correct ground-state spin for ^{10}B .

We mentioned earlier that already at the N^2LO order of the chiral perturbation theory the three-body terms appear. Those terms were not used in this work. However, work on their inclusion in the NCSM is under way [18]. It is reasonable to expect that these three-body terms will resolve the ^{10}B ground state problem. Structure of some of the EFT three-body terms in fact coincides with, e.g., the Tucson-Melbourne $\text{TM}'(99)$ three-nucleon interaction [37] that was already shown to resolve the ^{10}B problem when combined with the AV8' NN potential.

VI. CONCLUSIONS

We calculated the properties of ^3H , ^4He , ^6Li , ^6He and ^{10}B using the accurate charge-dependent NN potential at fourth order of chiral perturbation theory. We applied the *ab initio* no-core shell model and a variational calculation in the harmonic oscillator basis. For ^6Li , we were able to reach the basis size of up to $16\hbar\Omega$ using an improved multi-shell (no-core) version of the shell model code ANTOINE. We obtained the ^6Li binding energy of 28.5(5) MeV and a converged excitation spectrum. Properties of ^{10}B were obtained using the same NN potential in basis spaces of up to $8\hbar\Omega$. Our results are consistent with results obtained by standard accurate NN potentials and demonstrate a deficiency of Hamiltonians consisting of only two-body terms. In addition to under binding compared to experiment for all investigated nuclei, we found the ^6Li 3^+0 excitation energy over-predicted by about 700 keV compared to experiment. For ^{10}B we found an incorrect ground state, 1^+0 , contrary to experimental 3^+0 .

We anticipate that most of these problems will be resolved by including three-body terms that appear already at the third order of the chiral perturbation theory. A work on including these terms in the NCSM is under way [18].

Finally, let us note that recently a new accurate non-local NN potential has been constructed that fits not only the two-nucleon data but also the binding energies of ^3H and ^3He without any need to introduce a three-body interaction [38]. As our calculations show, the deficiencies of two-nucleon interactions are not limited only to the under binding but also to the nuclear structure issues most likely linked to an insufficient spin-orbit interaction strength. It will be very interesting to perform nuclear structure calculations using the new non-local NN potential of Ref. [38] to test its predictions for the binding energies and also for the spin-orbit interaction strength sensitive observables.

VII. ACKNOWLEDGMENTS

We thank R. Machleidt for providing the N^3LO NN potential code. We also thank A. Nogga for providing the ^4He N^3LO binding energy result obtained by the Faddeev-Yakubovsky method, K. Varga and W. Leidemann for the permission to present their ^6Li binding energy results for the Minnesota NN potential prior to publication. This work was partly performed under the auspices of the U. S. Department of Energy by the University of California, Lawrence Livermore National Laboratory under contract No. W-7405-Eng-48.

-
- [1] S. Weinberg, *Physica* **96A**, 327 (1979); *Phys. Lett. B* **251**, 288 (1990); *Nucl. Phys.* **B363**, 3 (1991).
 - [2] C. Ordonez, L. Ray, and U. van Kolck, *Phys. Rev. Lett.* **72**, 1982 (1994); *Phys. Rev. C* **53**, 2086 (1996).
 - [3] U. van Kolck, *Prog. Part. Nucl. Phys.* **43**, 337 (1999).
 - [4] E. Epelbaum, W. Glöckle, and Ulf-G. Meissner, *Nucl. Phys.* **A637**, 107 (1998); **A671**, 295 (2000).
 - [5] D. R. Entem and R. Machleidt, *Phys. Rev. C* **68**, 041001(R) (2003).
 - [6] R. B. Wiringa, V. G. J. Stoks and R. Schiavilla, *Phys. Rev. C* **51**, 38 (1995).
 - [7] R. Machleidt, *Phys. Rev. C* **63**, 024001 (2001).
 - [8] J.L. Friar, G.L. Payne, V.G.J. Stoks, and J.J. de Swart, *Phys. Lett. B* **311**, 4 (1993); W. Glöckle and H. Kamada, *Phys. Rev. Lett.* **71**, 971 (1993).
 - [9] R. B. Wiringa, S. C. Pieper, J. Carlson, V. R. Pandharipande, *Phys. Rev. C* **62**, 014001 (2000).

	NCSM ^a	Faddeev ^b	Yakubovsky ^c	Exp
³ H	-7.85(1)	-7.85	-	-8.48
⁴ He	-25.36(4)	-	-25.41	-28.30

^a This work
^b Ref. [20]
^c Ref. [18]

TABLE I: Calculated ³H and ⁴He ground state energies, in MeV, using the N³LO NN potential are compared to experiment.

- [10] S. C. Pieper, V. R. Pandharipande, R. B. Wiringa and J. Carlson, Phys. Rev. C **64**, 014001 (2001); S. C. Pieper and R. B. Wiringa, Ann. Rev. Nucl. Part. Sci. **51**, 53 (2001).
- [11] S. C. Pieper, K. Varga and R. B. Wiringa, Phys. Rev. C **66**, 044310 (2002); R. B. Wiringa and S. C. Pieper, Phys. Rev. Lett. **89**, 182501 (2002).
- [12] B. S. Pudliner, V. R. Pandharipande, J. Carlson, S. C. Pieper and R. B. Wiringa, Phys. Rev. C **56**, 1720 (1997).
- [13] P. Navrátil, J. P. Vary and B. R. Barrett, Phys. Rev. Lett. **84**, 5728 (2000); Phys. Rev. C **62**, 054311 (2000).
- [14] E. Caurier, G. Martínez-Pinedo, F. Nowacki, A. Poves, J. Retamosa and A. P. Zuker, Phys. Rev. C **59**, 2033 (1999); E. Caurier and F. Nowacki, Acta Physica Polonica **30**, 705 (1999).
- [15] E. Caurier, P. Navrátil, W. E. Ormand and J. P. Vary, Phys. Rev. C **64**, 051301 (2001).
- [16] E. Epelbaum, A. Nogga, W. Glöckle, H. Kamada, Ulf-G. Meissner and H. Witala, Phys. Rev. C **66**, 064001 (2002).
- [17] P. Navrátil and W. E. Ormand, Phys. Rev. C **68**, 034305 (2003).
- [18] A. Nogga, private communication.
- [19] H. J. Lipkin, Phys. Rev. **109**, 2071 (1958).
- [20] R. Machleidt, private communication.
- [21] U. van Kolck, Phys. Rev. C **49**, 2932 (1994).
- [22] P. Navrátil and B. R. Barrett, Phys. Rev. C **59**, 1906 (1999).
- [23] P. Navrátil, G. P. Kamuntavičius and B. R. Barrett, Phys. Rev. C **61**, 044001 (2000).
- [24] K. Suzuki and S. Y. Lee, Prog. Theor. Phys. **64**, 2091 (1980).
- [25] K. Suzuki, Prog. Theor. Phys. **68**, 246 (1982).
- [26] D. R. Thomson, M. LeMere and Y. C. Yang, Nucl. Phys. **A286**, 53 (1977).
- [27] K. Varga and Y. Suzuki, Phys. Rev. C **52**, 2885 (1995).
- [28] N. Barnea, W. Leidemann and G. Orlandini, Phys. Rev. C **67**, 054003 (2003).
- [29] K. Varga, private communication.
- [30] N. Barnea, W. Leidemann and G. Orlandini, Phys. Rev. C **61**, 054001 (2000); Nucl. Phys. **A693**, 565 (2001);
- [31] W. Leidemann, private communication.
- [32] P. Navrátil, J. P. Vary, W. E. Ormand and B. R. Barrett, Phys. Rev. Lett. **87**, 172502 (2001).
- [33] P. Navrátil and W. E. Ormand, Phys. Rev. Lett. **88**, 152502 (2002).
- [34] R. Schiavilla and R. B. Wiringa, Phys. Rev. C **65**, 054302 (2002).
- [35] I. Stetcu, private communication.
- [36] E. Caurier, P. Navrátil, W. E. Ormand and J. P. Vary, Phys. Rev. C **66**, 024314 (2002).
- [37] S. A. Coon and H. K. Han, Few-Body Systems **30**, 131 (2001).
- [38] P. Doleschall, I. Borbély, Z. Papp and W. Plessas, Phys. Rev. C **67**, 064005 (2003).
- [39] F. Ajzenberg-Selove, Nucl. Phys. A **490**, 1 (1988).
- [40] D. R. Tilley, C. M. Cheves, J. L. Godwin, G. M. Hale, H. M. Hofmann, J. H. Kelley, C. G. Sheu and H. R. Weller, Nucl. Phys. A **708**, 3 (2002).

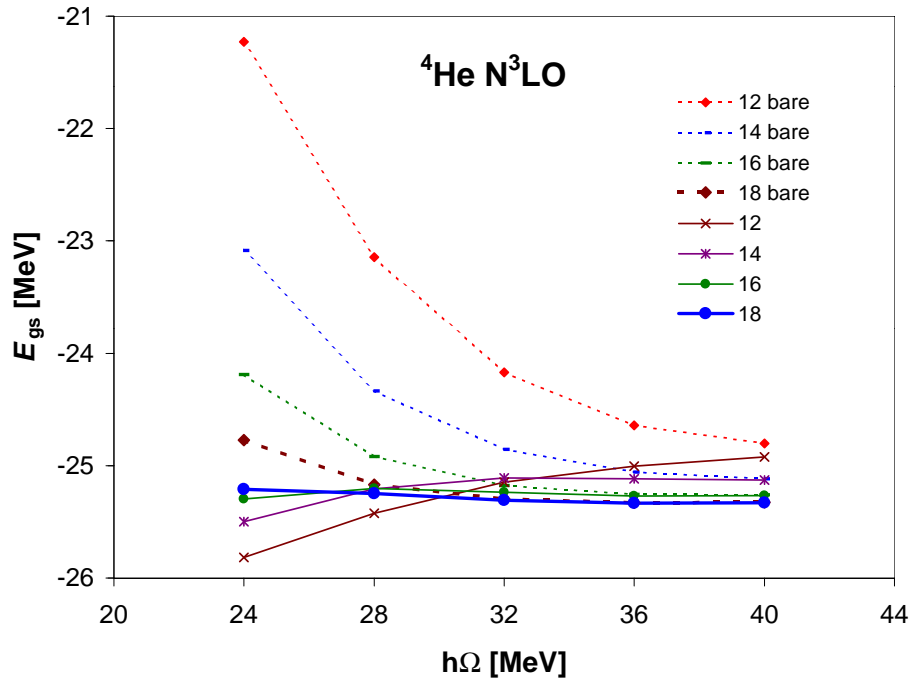


FIG. 1: (Color online) Harmonic-oscillator frequency dependence of the ${}^4\text{He}$ ground-state energy obtained in $12\hbar\Omega$ - $18\hbar\Omega$ ($N_{\text{max}} = 12 - 18$) basis spaces using the bare N^3LO NN potential (dotted lines) and two-body effective interactions derived from the N^3LO NN potential (full lines). The Coulomb potential is included.

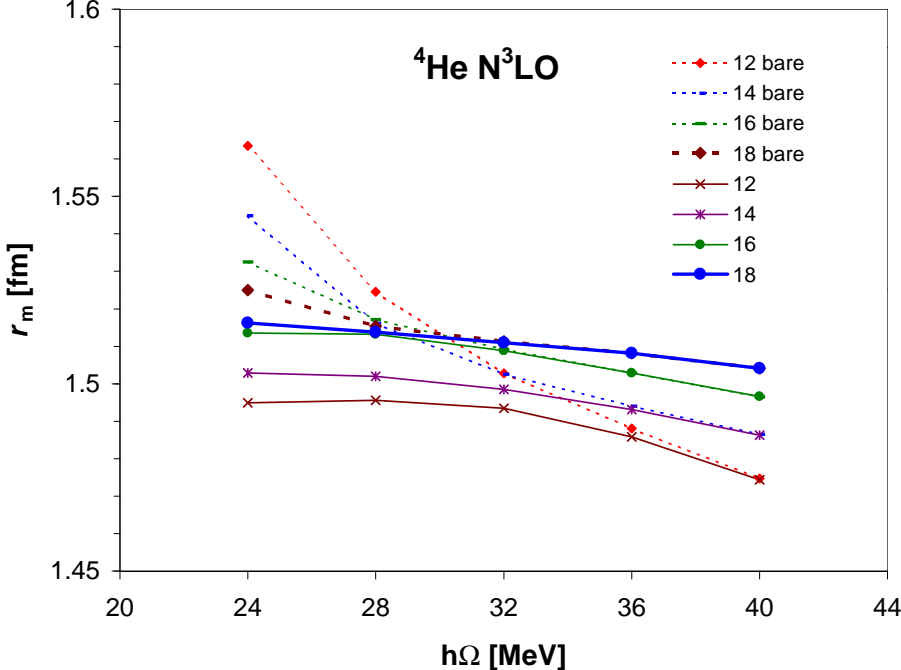


FIG. 2: (Color online) The same as in Fig. 1 for the point-nucleon radius.

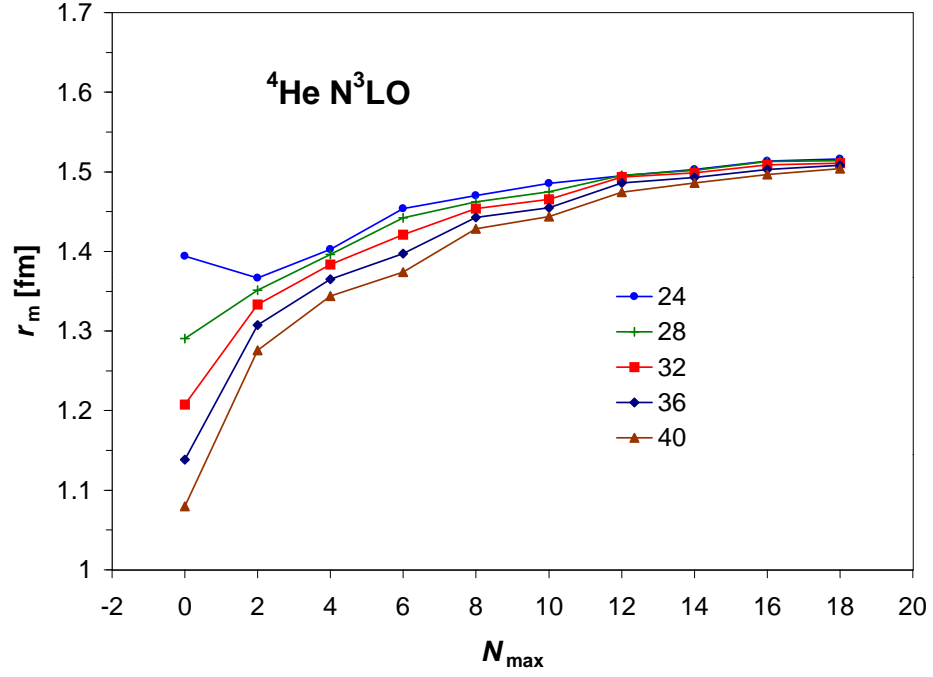


FIG. 3: (Color online) Basis size dependence of the ${}^4\text{He}$ point-nucleon radius obtained using the two-body effective interactions derived from the N^3LO NN potential. Results for the harmonic-oscillator frequencies $\hbar\Omega = 24, 28, 32, 36, 40$ MeV are presented.

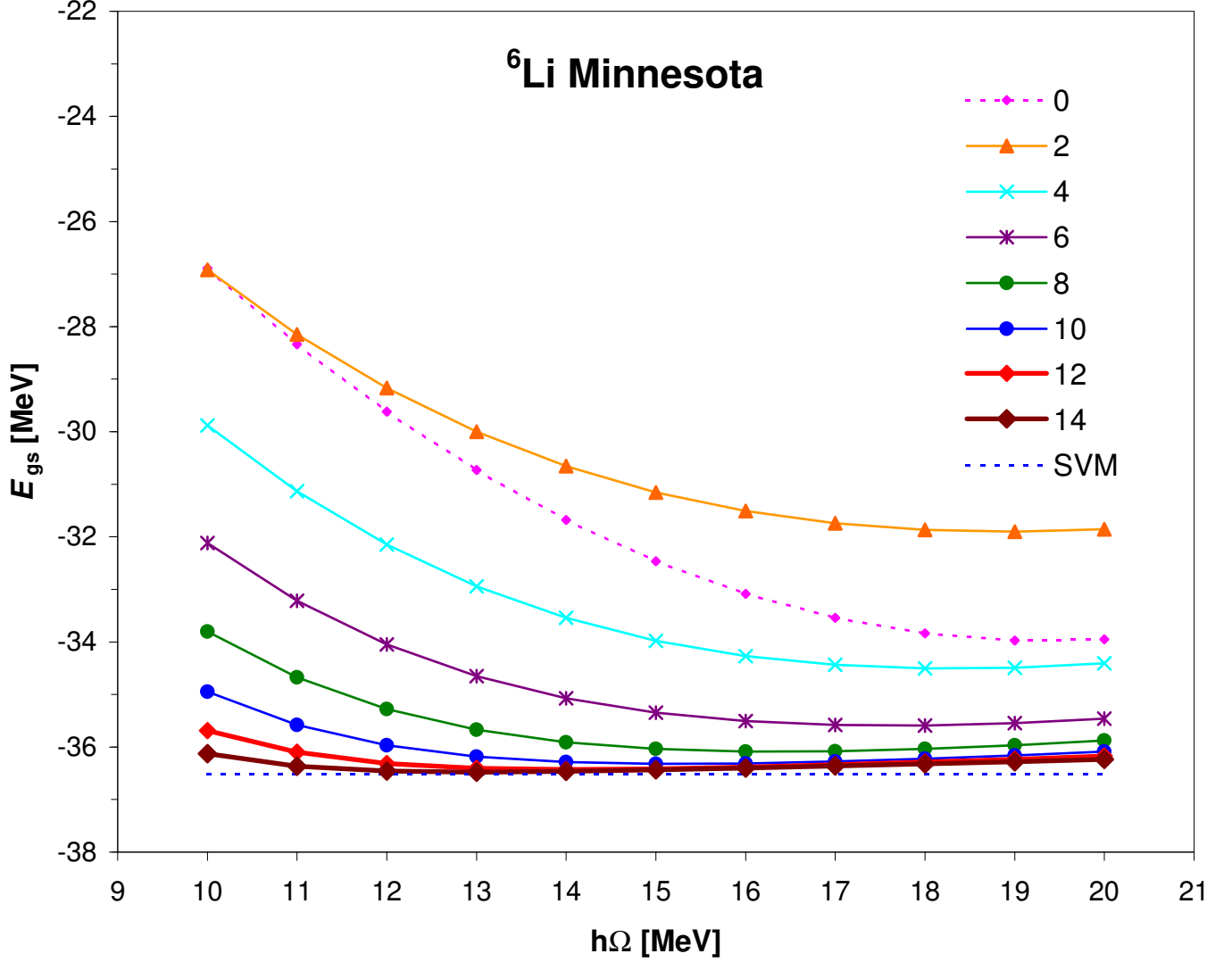


FIG. 4: (Color online) Harmonic-oscillator frequency dependence of the ${}^6\text{Li}$ ground-state energy obtained in $0\hbar\Omega$ - $14\hbar\Omega$ basis spaces using two-body effective interactions derived from the Minnesota NN potential. Coulomb potential is not included. The dotted line corresponds to the Stochastic Variational Method result [29].

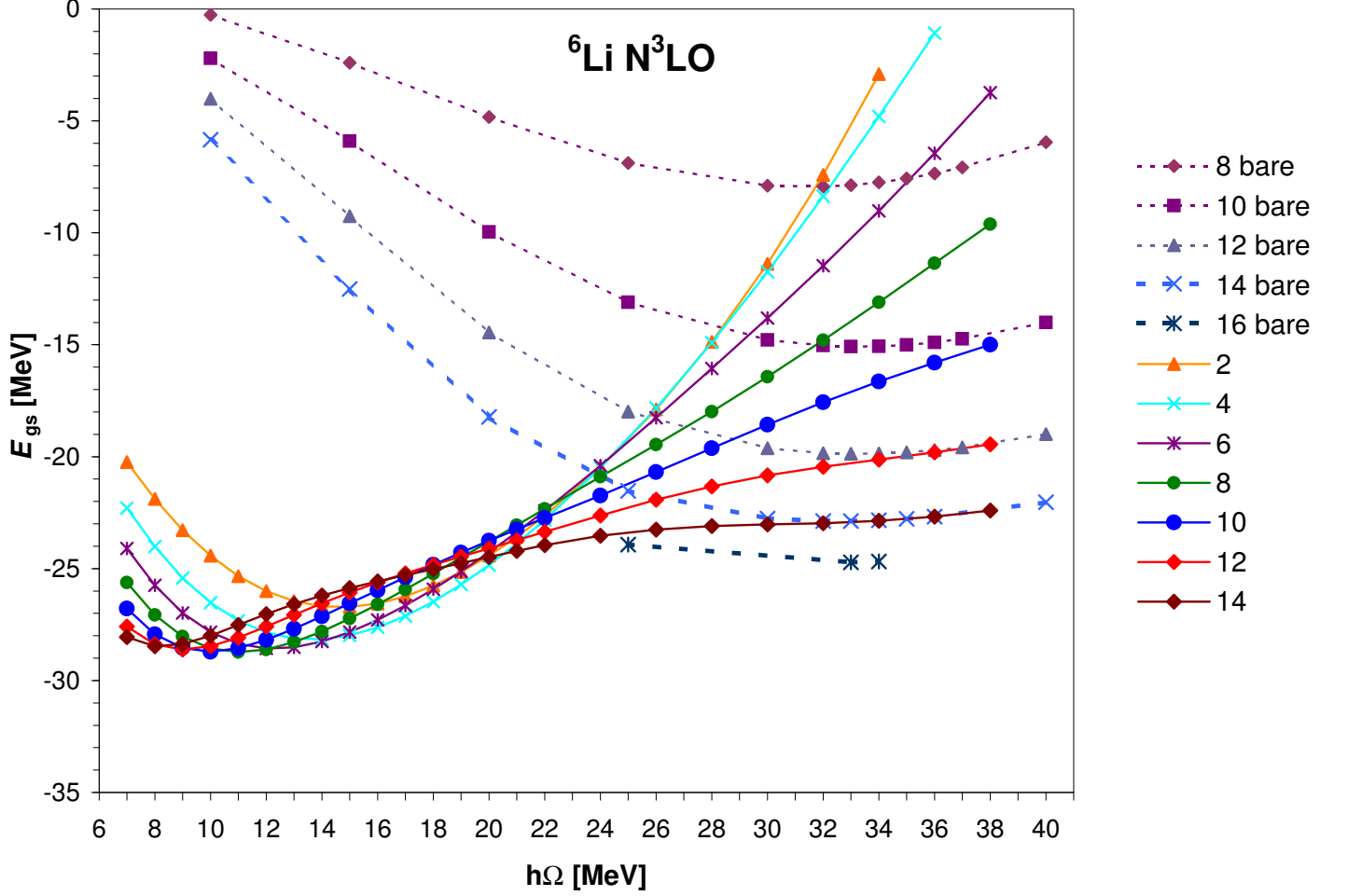


FIG. 5: (Color online) Harmonic-oscillator frequency dependence of the ${}^6\text{Li}$ ground-state energy obtained in $2\hbar\Omega$ - $14\hbar\Omega$ and $8\hbar\Omega$ - $16\hbar\Omega$ basis spaces using two-body effective interactions derived from the $N^3\text{LO}$ NN potential (full lines) and the bare $N^3\text{LO}$ NN potential (dotted lines), respectively. The Coulomb potential is included.

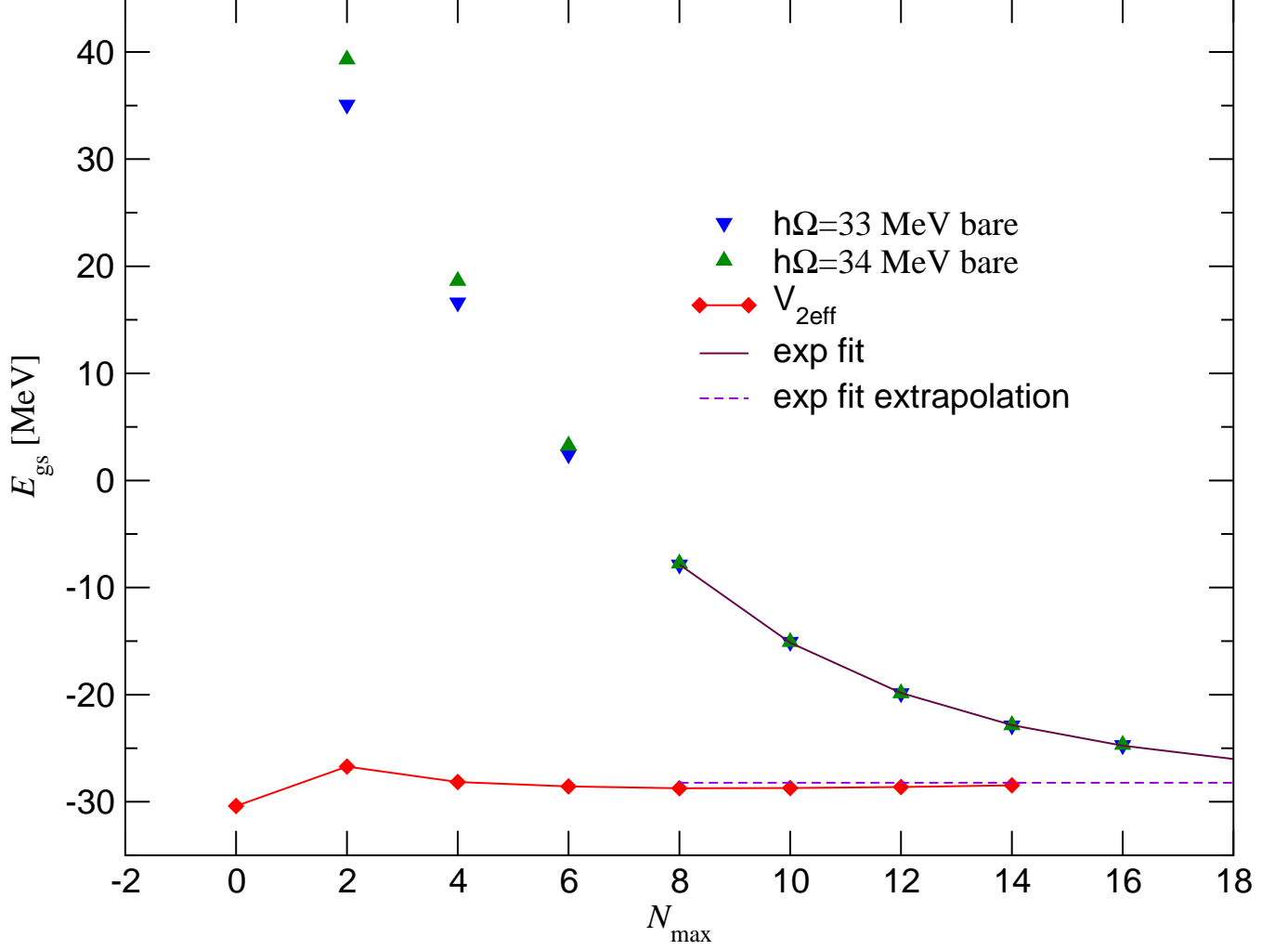


FIG. 6: (Color online) Basis size dependence of the ${}^6\text{Li}$ ground-state energy obtained in $0\hbar\Omega$ - $14\hbar\Omega$ and $0\hbar\Omega$ - $16\hbar\Omega$ basis spaces using two-body effective interactions derived from the $N^3\text{LO}$ NN potential and the bare $N^3\text{LO}$ NN potential, respectively. The Coulomb potential is included. The two-body effective interaction results correspond to the ground-state energy minimum for each model space. For details on the extrapolation see the text.

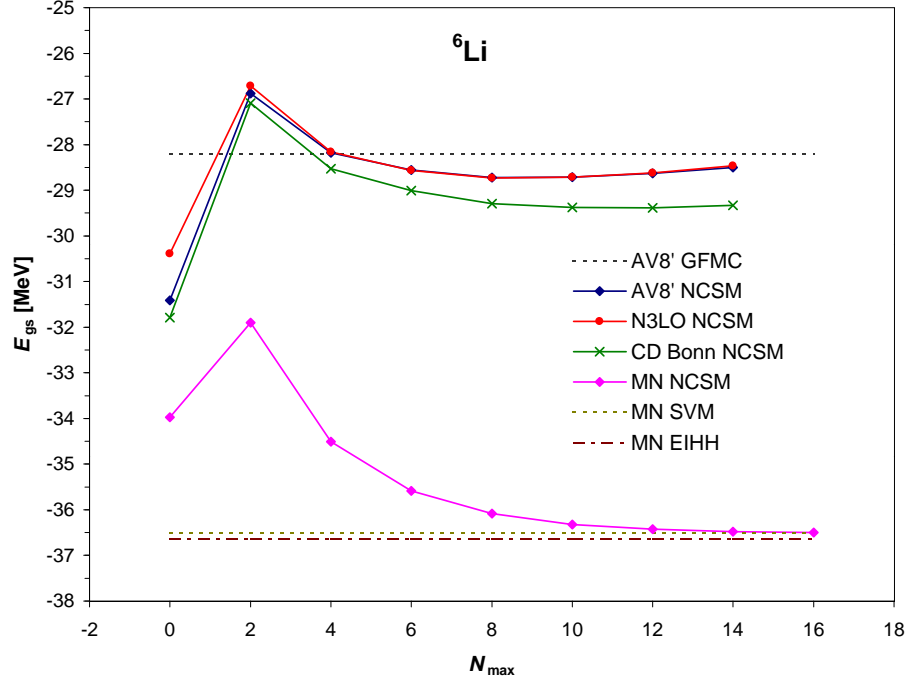


FIG. 7: (Color online) Basis size dependence of the ${}^6\text{Li}$ ground-state energy obtained in $0\hbar\Omega$ - $14\hbar\Omega$ ($16\hbar\Omega$ for MN) basis spaces using two-body effective interactions derived from the AV8', N³LO, CD-Bonn 2000 and the Minnesota NN potentials. The AV8' result obtained by the GFMC method [10] and the Minnesota results obtained by the SVM [29] and the EIHH methods [31] are shown for a comparison.

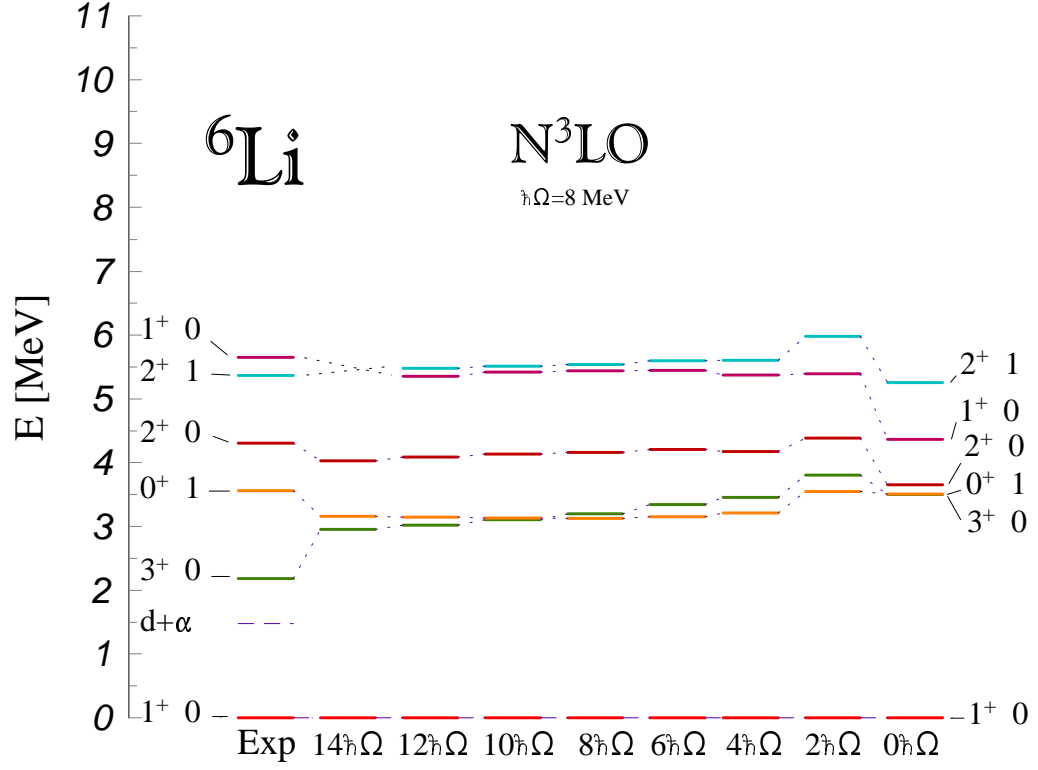


FIG. 8: (Color online) Calculated positive-parity excitation spectra of ${}^6\text{Li}$ obtained in $0\hbar\Omega$ - $14\hbar\Omega$ ($12\hbar\Omega$ for the 2^+1 and 1^+_{20} states) basis spaces using two-body effective interactions derived from the N^3LO NN potential are compared to experiment. The HO frequency of $\hbar\Omega = 8 \text{ MeV}$ was used. The experimental values are from Ref. [39].

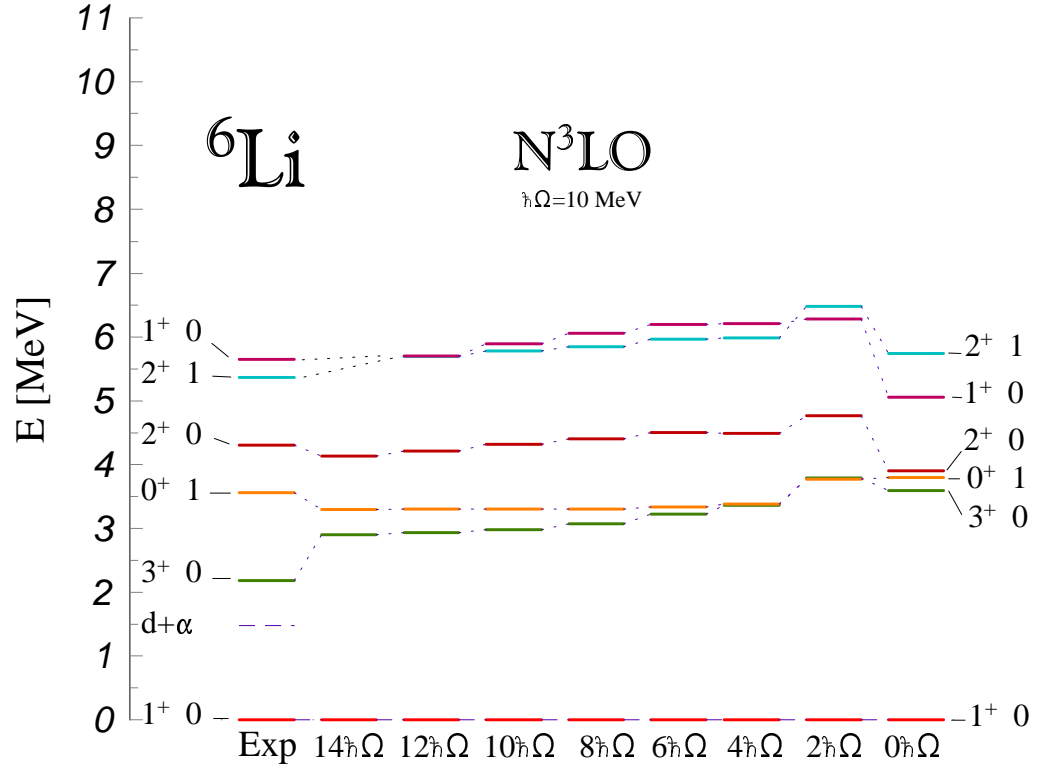


FIG. 9: (Color online) The same as in Fig. 8 for the HO frequency of $\hbar\Omega = 10 \text{ MeV}$.

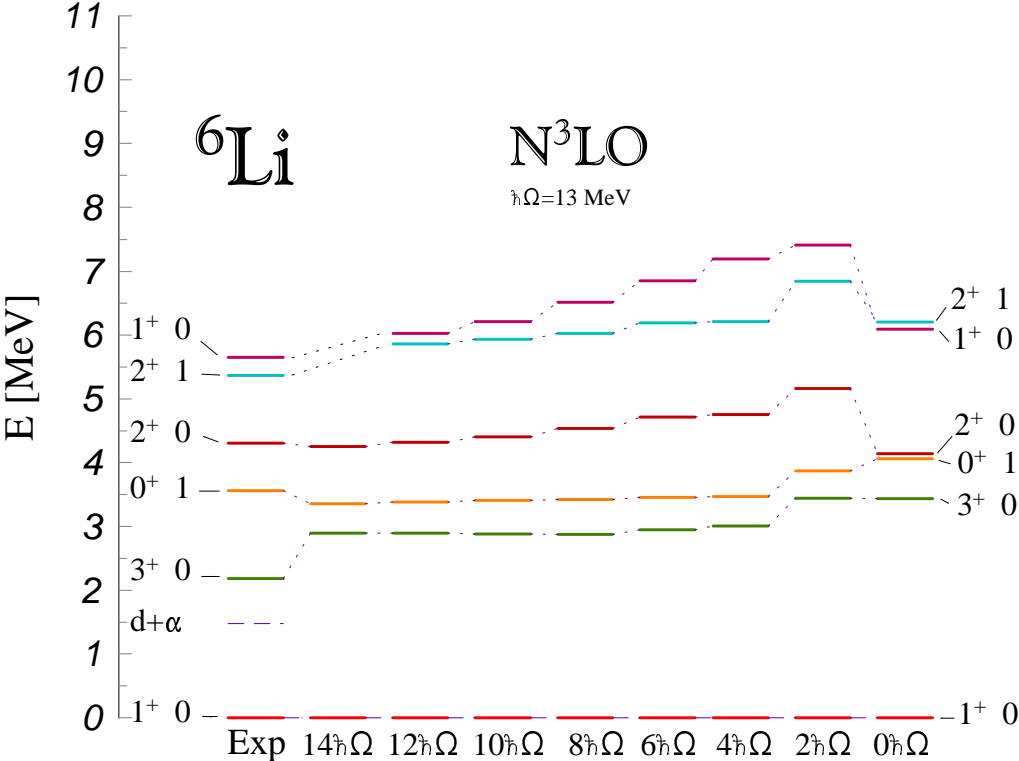


FIG. 10: (Color online) The same as in Fig. 8 for the HO frequency of $\hbar\Omega = 13 \text{ MeV}$.

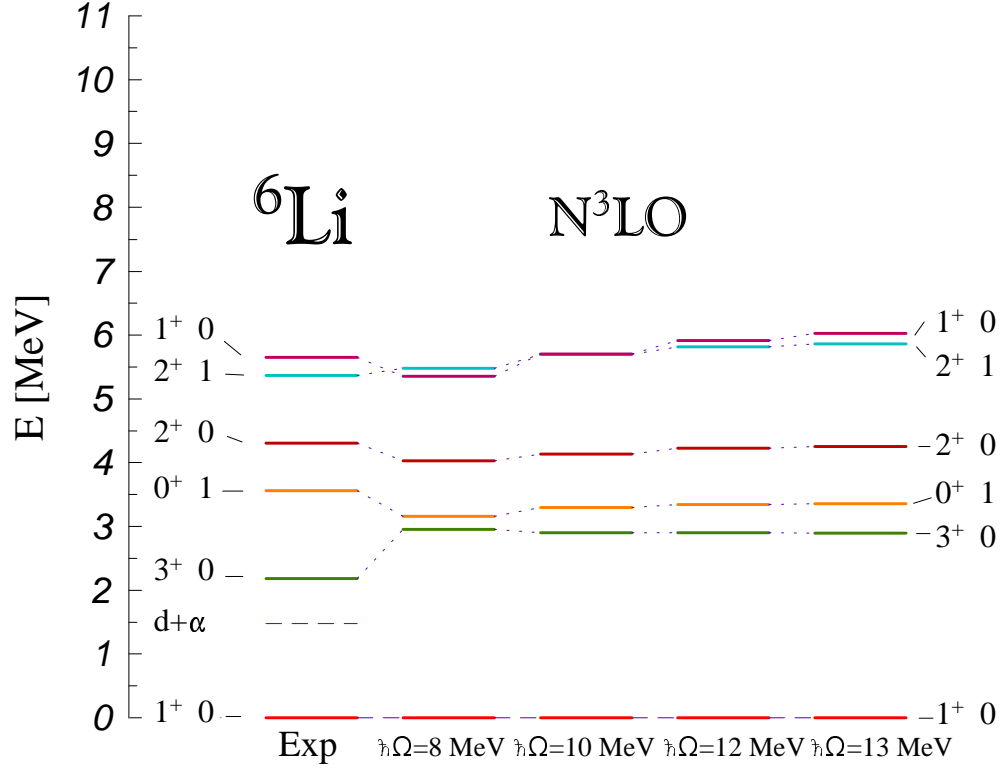


FIG. 11: (Color online) Calculated positive-parity excitation spectra of ${}^6\text{Li}$ obtained in the $14\hbar\Omega$ ($12\hbar\Omega$ for the 2^+1 and $1^+_{\frac{1}{2}}0$ states) basis space using two-body effective interactions derived from the N^3LO NN potential are compared to experiment. The HO frequency dependence in the range of $\hbar\Omega = 8 - 13$ MeV is presented. The experimental values are from Ref. [39].

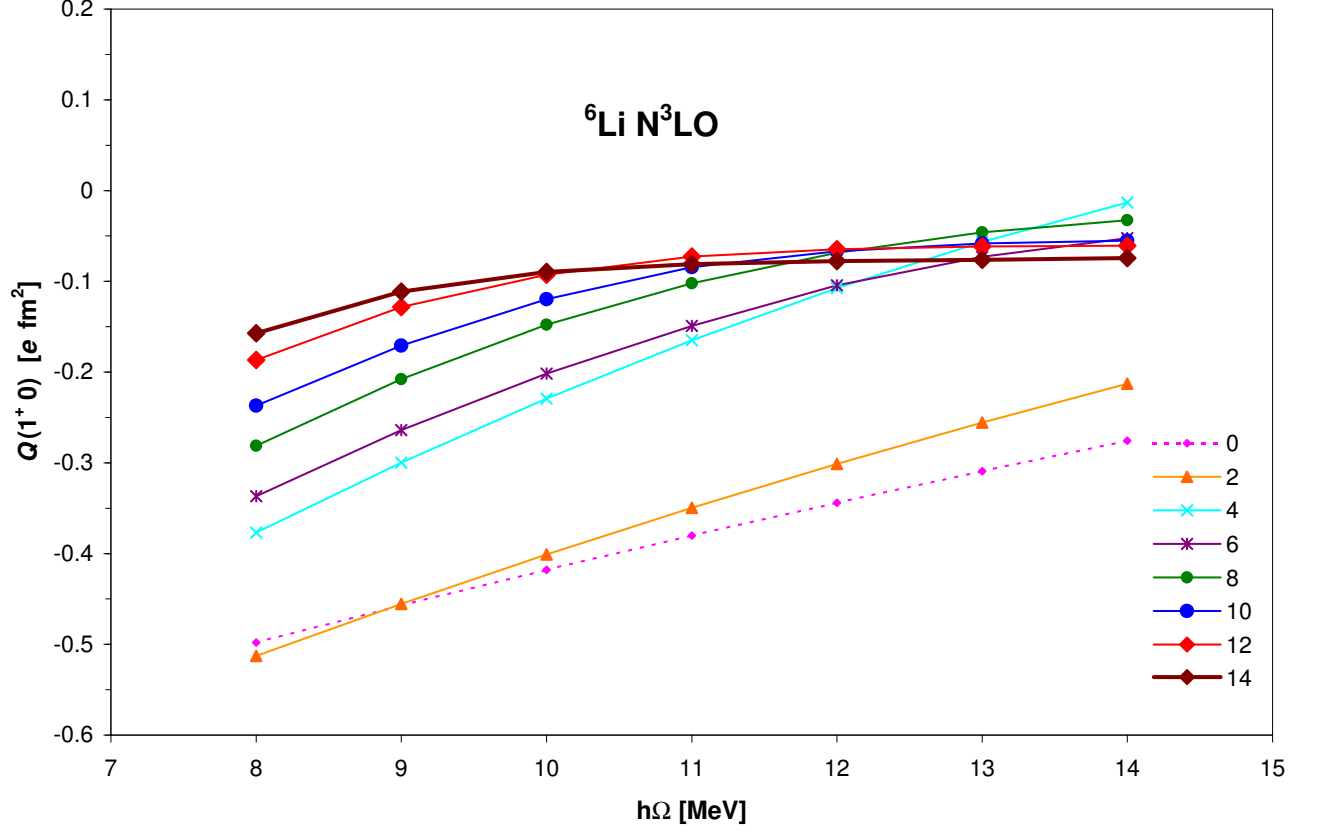


FIG. 12: (Color online) Harmonic-oscillator frequency dependence of the ${}^6\text{Li}$ quadrupole moment obtained in $0\hbar\Omega$ - $14\hbar\Omega$ ($N_{\max} = 0 - 14$) basis spaces using two-body effective interactions derived from the $N^3\text{LO}$ NN potential.

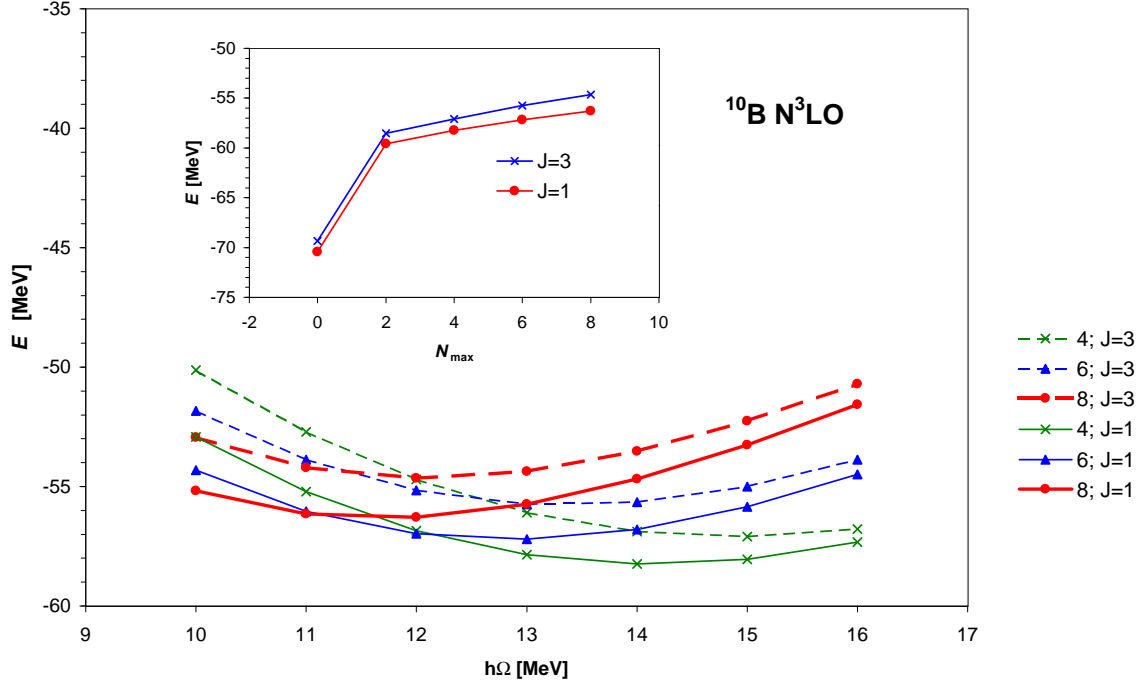


FIG. 13: (Color online) The dependence of the ^{10}B 1^+0 and 3^+0 state energy on the HO frequency for the $4\hbar\Omega$, $6\hbar\Omega$ and $8\hbar\Omega$ model spaces calculated using the N^3LO NN potential. In the inset, the 1^+0 and 3^+0 state energies at their respective HO frequency minima are plotted as a function of N_{max} .

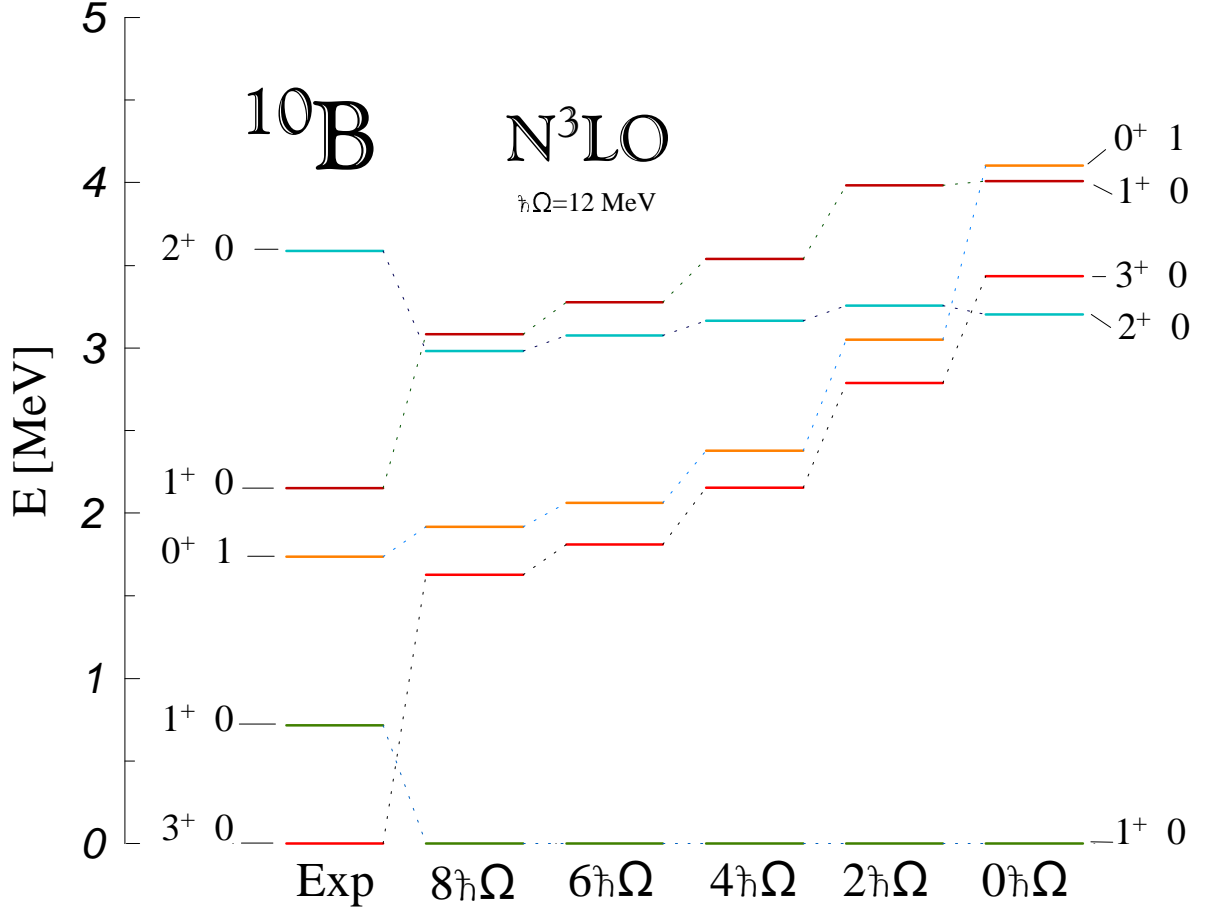


FIG. 14: (Color online) Calculated positive-parity excitation spectra of ^{10}B obtained in $0\hbar\Omega$ - $8\hbar\Omega$ basis spaces using two-body effective interactions derived from the $N^3\text{LO}$ NN potential are compared to experiment. The HO frequency of $\hbar\Omega = 12\text{ MeV}$ where the $8\hbar\Omega$ ground state is at the minimum was used. The experimental values are from Ref. [39].

${}^6\text{Li}$	Exp	N ³ LO
$ E_{\text{gs}} (1^+0)$	31.995	28.5(5)
$Q_{\text{gs}} [e \text{ fm}^2]$	-0.082(2)	-0.08(2)
$\mu_{\text{gs}} [\mu_N^2]$	+0.822	+0.839(5)
$E_x(1_1^+0)$	0.0	0.0
$E_x(3^+0)$	2.186	2.91(3)
$E_x(0^+1)$	3.563	3.30(10)
$E_x(2^+0)$	4.312	4.10(15)
$E_x(2_1^+1)$	5.366	5.50(30)
$E_x(1_2^+0)$	5.65	5.40(30)
B(E2; $1_1^+0 \rightarrow 3^+0$)	21.8(4.8)	16.0(1.5)
B(M1; $0^+1 \rightarrow 1_1^+0$)	15.42(32)	15.01(10)
B(E2; $2^+0 \rightarrow 1_1^+0$)	4.41(2.27)	6.2(8)
<hr/>		
${}^6\text{He}$	Exp	N ³ LO
$ E_{\text{gs}} (0^+1)$	29.269	26.2(5)
<hr/>		
${}^6\text{He} \rightarrow {}^6\text{Li}$	Exp	N ³ LO
B(GT; $0_1^+1 \rightarrow 1_1^+0$)	4.728(15)	5.22(10)

TABLE II: Experimental and calculated energies, in MeV, quadrupole and magnetic moments, as well as E2, in $e^2 \text{ fm}^4$, and M1, in μ_N^2 , transitions of ${}^6\text{Li}$ and ${}^6\text{He}$ as well as the B(GT) values for the ${}^6\text{He}$ ground state to ${}^6\text{Li}$ ground state transition. Results obtained using the N³LO NN potential are presented. The errors are estimated from the HO frequency and basis size dependences as well as the bare interaction result extrapolations. The experimental values are from Ref. [39, 40].

	Exp	NCSM N ³ LO	NCSM CD-Bonn	NCSM AV8'	GFMC AV8'	NCSM MN	SVM MN	EIHH MN
$ E_{\text{gs}} (1^+0)$	31.995	28.5(5)	29.35(40)	28.5(5)	28.19(5)	36.50(4)	36.51	36.64(7)
$E_x(1^+0)$	0.0	0.0	0.0	0.0	0.0			
$E_x(3^+0)$	2.186	2.91(3)	2.86	2.97	3.21(7)			
$E_x(0^+1)$	3.563	3.30(10)	3.29	3.41	3.94(8)			
$E_x(2^+0)$	4.312	4.10(15)	4.47	4.28	4.10(6)			

TABLE III: Experimental and calculated energies, in MeV, of ${}^6\text{Li}$. Binding and excitation state energy results for the realistic N³LO, CD-Bonn 2000, AV8' NN potentials and the binding energy for the semi-realistic Minnesota (without Coulomb) NN potential are presented. The GFMC [10], the SVM [29] and the EIHH [31] results are shown for comparison. See the text for further details.

${}^{10}\text{B}$	Exp	N ³ LO
$ E(3^+0) $	64.751	54.65
$ E(1^+0) $	64.033	56.28
$E_x(3_1^+0)$	0.0	0.0
$E_x(1_1^+0)$	0.718	-1.628
$E_x(0_1^+1)$	1.740	0.293
$E_x(1_2^+0)$	2.154	1.459
$E_x(2_1^+0)$	3.587	1.356

TABLE IV: Experimental and calculated energies, in MeV, of ${}^{10}\text{B}$. The NCSM results obtained using the two-body effective interaction derived from the N³LO NN potential in the $8\hbar\Omega$ basis space and the HO frequency of $\hbar\Omega = 12 \text{ MeV}$. The experimental values are from Ref. [39]